Proceedings of
ASME TURBO EXPO 2001
June 4-7, 2001, New Orleans, Louisiana

2001-GT-0592

EFFECT OF THE AXIAL SPACING BETWEEN ROTOR AND STATOR WITH REGARD TO THE INDEXING IN AN AXIAL COMPRESSOR

M. Y. Layachi
Swiss Federal Institute of Technology
EPFL-LTT
Lausanne, Switzerland

A. Bölcs
Swiss Federal Institute of Technology
EPFL-LTT
Lausanne, Switzerland

ABSTRACT

An experimental investigation was carried out to examine the influence of the axial spacing between rotor and stator. The test facility of the Swiss Federal Institute of Technology is made up of an inlet guide vane (IGV), a rotor and a stator. Temperature and aerodynamic measurements determined the characteristics of the compressor stage. Data were acquired over a range of flow coefficients for four different axial spacings. A refined measurement mesh was used for Pitot probe measurements in different sections of the compressor. As the compressor has a rather low aspect ratio of 1.21, the flow was governed by strong secondary flows. The interaction between the different secondary flows, especially the Influence of the IGV wake on the secondary flows in the stator, were detected by the detailed Pitot probe measurements. Shifting the stator axially changes the circumferential position of the IGV wake entering the stator. From this statement, the link between an axial variation of the distance between rotor and stator and the clocking between IGV and stator will be shown. Further Pitot measurement with different indexings between IGV and stator were performed. The Pitot measurements for the different axial spacings as for the different indexings brought to light strong interactions in the wall regions especially between the IGV wake and the clearances at the rotor tip and at the stator hub. The structure of the flow thus changes with the indexing and with the axial spacing.

1. INTRODUCTION

In 1969 Leroy H. Smith investigated the casing boundary layer effects in a four-stage axial compressor [ref. 1]. He noticed a slight improvement in the efficiency and static pressure rise coefficient, over the whole range of studied flow coefficient, when the axial spacing was decreased from $\xi/h=0.174$ to $\xi/h=0.033$. In 1975 Hetherington and Moritz [ref. 3] found the opposite trend. They noticed an improvement of the characteristics for a four-stage axial compressor when increasing the gap by a factor 4. They also showed the effect of the inlet guide vane on the compressor characteristics. Below a certain Mach number, the efficiency is increased by the removal of the inlet guide vane. Above, the efficiency deteriorates compared to the case with inlet guide vane. However, these studies do not take into account the effect of the circumferential positions of the IGV relative to the stator (i.e. the indexing). Only in the last decade, experimenters have investigated this parameter. Barankiewicz and Hathaway investigated the overall performances on the NASA Lewis test facility for a four-stage low speed axial compressor when varying the indexation between the stator rows. For both peak efficiency and peak pressure rise operating conditions, the indexing was performed by measuring the wake position of the upstream stator at the inlet of the following stator row. Hence, a flow dependent indexing was performed for the two flow conditions. The impact of stator indexing on compressor performance was found to be small. However the low velocity used in their test (c_x=24.4 m/s) does not favor the action of the secondary flows involved when varying the indexing. Using an unsteady, quasi-three-dimensional Navier-Stokes analysis, applied to a high-speed axial compressor, Dorney et al. [ref. 6] showed that stator clocking can result in efficiency gain of 0.6-0.7%. The highest efficiency is observed when the wake of the first stage stator flows onto the pressure surface of the second stage stator. The momentum thickness and skin friction were found to be greater on the second stage at the highest efficiency conditions. Hubert and all. [ref. 8, ref. 9] showed that 0.8 percent point improvement was possible when varying the indexing between turbine airfoils.

In the above indexing investigations, the effects of the secondary flows near the walls were not mentioned.
This paper addresses the influence of the axial variation of the spacing between the rotor and the stator on the characteristics of the compressor stage and on the flow structure. It will show the link between the axial spacing between airfoil rows and indexings. It will also show the influence of the axial distance between the rotor and the stator, and of the indexing between the IGV and the stator on the flow structure in the endwall regions.

2. TEST FACILITY AND MEASUREMENT EQUIPMENT

2.1 The test Facility

The compressor test facility of the LTT (Laboratoire de Thermique appliquée et de Turbomachines) is made up of an inlet guide vane (IGV), a rotor, and a stator. An electric motor drives the rotor to a tip velocity up to 226 m/s. The test facility is a closed loop, which enables the use of gases other than air. The temperature is held constant with the aid of heat exchangers (Fig. 1). The hub diameter is 160 mm and the channel height is 40 mm.

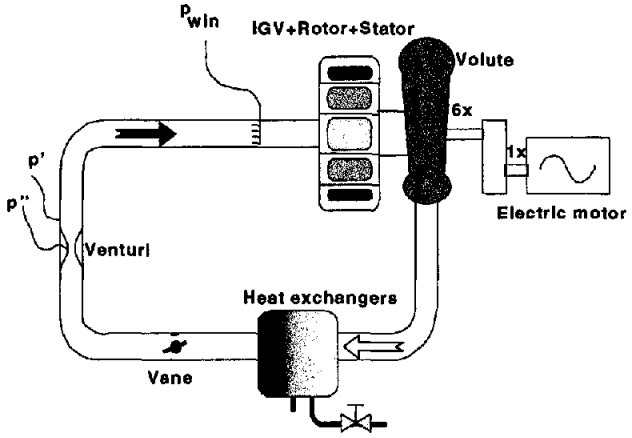

Fig. 1 Closed loop axial compressor test facility

For this study the test facility was set up in order to vary the axial spacing between the rotor and the stator, by means of distance rings on the casing. These rings of different thicknesses mounted upwind or downwind the stator, enable the following axial spacings: ξ/h= 6.25 %, 9.5 %, 12.5% and 18.75 %. The rotor tip clearance and the trailing stator hub clearance were held constant for this study to a value of t/h=1.25%. The IGV is sealed at hub and tip.

Traverses are accomplished by moving the IGV and the stator in unison past stationary probes mounted on radial actuators attached to the fixed tight chamber around the casing. The rotation is performed with the aid of a hydraulic cylinder. The indexing between the IGV and the stator is performed with a second hydraulic cylinder mounted between the IGV and the stator. The activation of this second cylinder will rotate the stator alone as the IGV will remain "frozen".
The test facility allows measurements with the aid of temperature and aerodynamic probes in the four following axial locations (Fig. 2):

- At the I.G.V. inlet,
- between the IGV and the rotor,
- between the rotor and the stator,
- 84% of axial chord downstream of the stator trailing edge.

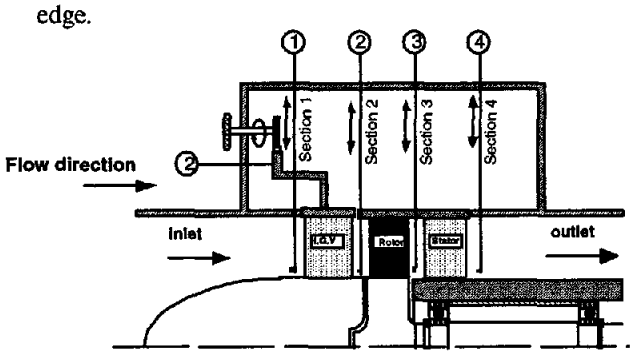

Fig. 2 Scheme of the test facility with the measurement sections.

2.2 Probes traverse measurements

Fig. 3 shows the measurement locations for the determination of the Characteristics of the compressor stage. Traverse measurements were performed in sections 1, 2 and 4. The flow being homogeneous in the pitchwise direction in section 1, a single radial traverse was performed at this location. In sections 2 and 4, the included measurement surface in each section goes from 10% to 90% of the span and the radial step was 4 mm (10% of channel height). In the pitchwise direction, the measurement surface covers 18 degrees, corresponding to the stator pitch. The resolution of the mesh for the first four degrees of the surface is of 0.5 degree, because of the presence of the IGV wake in section 2. The rest of the surface was measured every degree. The inlet stagnation temperature was kept constant to a value of T_c= 293°K±0.2°K.

Nomenclature

c_x	Axial velocity
L_{xstat}	Axial stator chord [mm]
T_c	Stagnation temperature [K]
h	Channel height [mm]
t	tip clearance [mm]
u	tangential velocity of the rotor at midspan
z	Radial coordinate [mm]
η_s	Isentropic efficiency
ξ	Axial spacing between rotor and stator [mm]
θ	pitchwise position / pitchwise step [degree]
θ_{stat}	Stator pitch [degree]
$\overline{\quad}t$	Pitchwise averaging

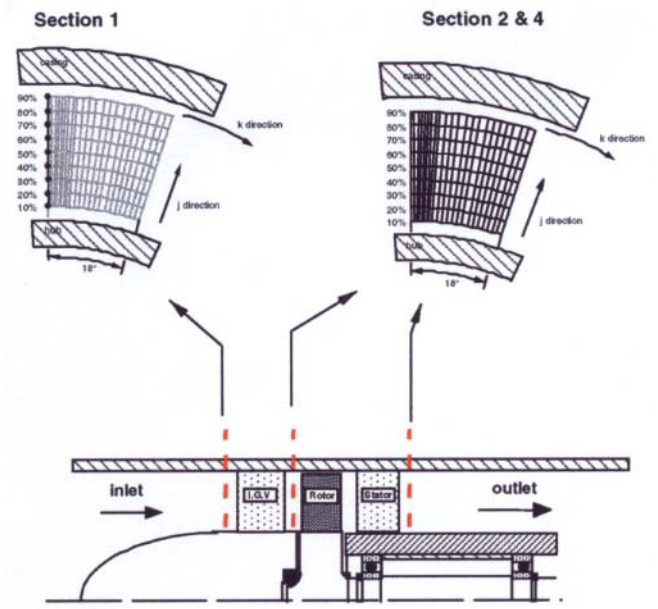

Fig. 3 Full traverse measurements

2.3 The Pitot Probes measurements

In order to have a detailed description of the loss zones for the different configurations of the compressor, measurements of the flow field were performed with cobra type Pitot probes on a refined mesh. These measurements were performed to identify the secondary flows and to determine their extent. The flow field is measured in sections 2 and 4, from 1% to 99% span and over a stator pitch (18 degrees). The measurement mesh has 79 points in the radial direction and 37 point in the pitchwise direction. The step in the pitchwise direction is 0.5 degrees. In the radial direction the step for the measurements is 1% of the channel height from z/h=1% to 30% and from z/h=70% to 99% of the channel height. The radial step in the other locations is 2% of the channel height. Fig. 4 shows this mesh having 2923 measurement points per section. The advantage of using a Pitot tube with a diameter of 0.95 mm is that it reduces the wall effects due to the presence of the probe.

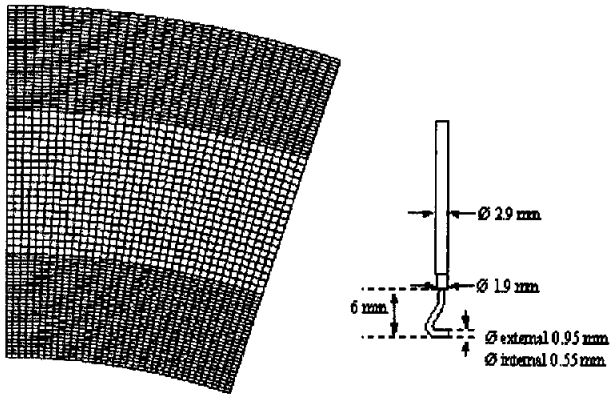

Fig. 4 Detailed measurement mesh made of 2923 nodes and the Pitot probe.

3. THE AXIAL SPACING

3.1 Probe traverse measurements

Four axial distances between rotor and stator were investigated. As the rotor blades are twisted, the position of the trailing edge varies with the radius. The axial spacing is defined at the hub and the investigated distances are listed in Table 1.

ξ [mm]	2.5	3.8	5.0	7.5
ξ/h	6.25 %	9.5 %	12.5%	18.75 %
ξ/L_{xsta}	9.2 %	14 %	18.4 %	27.6 %

Table 1 Values of the studied axial spacings

The isentropic efficiency calculated with the stagnation pressures and temperatures issued from the probe measurements in section 2 and 4 is plotted in Fig. 5 for the investigated axial spacings. There is no trend with the axial spacing, concerning the efficiency.

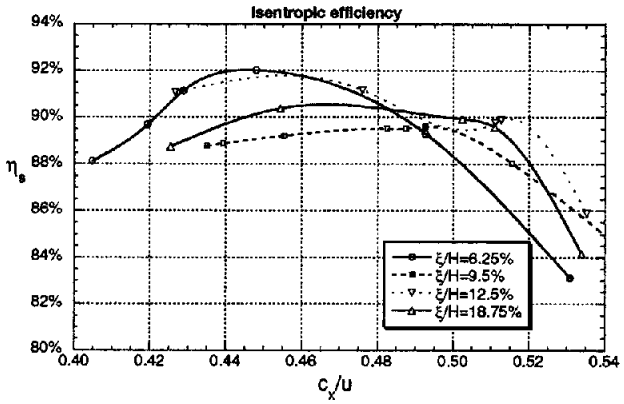

Fig. 5 Isentropic efficiency of the compressor stage for the four axial spacings.

Comparisons of pitchwise distribution of the stagnation pressure between the four axial spacings were done for *"near design"* and *"high-loaded"* flow conditions. The comparisons were done at hub, midspan and casing. In order to compare the radial distribution of the flow pattern, the stagnation pressure ratio was mass averaged in the pitchwise direction. All these results were issued from the measurements performed with the aerodynamic and temperature probes. The test cases used are listed in Table 2. A slight correction was done on some of the measurement in order to adjust the levels to the desired flow coefficient. Care was taken to choose cases that had flow coefficients close to each other.

For the large flow coefficient of about $c_x/u=0.53$, the distributions of the Mach number (Fig. 6) and of the stagnation pressure distribution in the section downstream of the stator do not seem to vary with the axial spacing.

However, when the loading is increased, a thicker wake is observed for $\xi/h=6.25\%$. When increasing the spacing to $\xi/h=9.5\%$, the wake position moves in the suction side

direction. From hub to midspan, this displacement corresponds to about 28% pitch.

	Test No	p_{c4}/p_{c2}	c_x/u
Low loading conditions			
ξ/h=6.25%	073	1.049	0.527
ξ/h=9.5%	191	1.050	0.541
ξ/h=12.5%	002	1.049	0.526
ξ/h=18.75%	163	1.050	0.528
Near design conditions			
ξ/h=6.25%	072	1.067	0.493
ξ/h=9.5%	171	1.060	0.516
ξ/h=12.5%	022	1.064	0.507
ξ/h=18.75%	165	1.065	0.507
High-loaded conditions			
ξ/h=6.25%	081	1.092	0.432
ξ/h=9.5%	176	1.093	0.433
ξ/h=12.5%	004	1.096	0.423
ξ/h=18.75%	162	1.095	0.424

Table 2 Test cases used for the comparisons

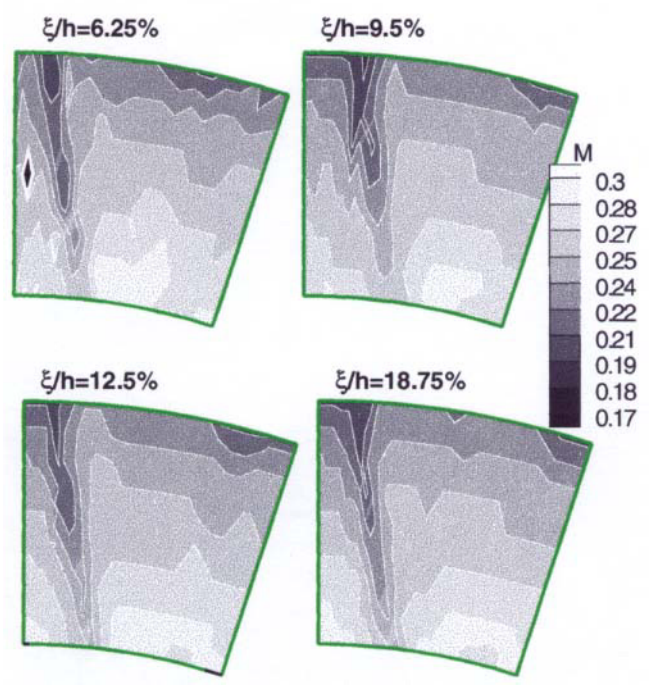

Fig. 6 Mach distribution downstream of the stator for the four axial spacings and for c_x/u~0.53 (low loading)

At high loaded conditions (c_x/u=0.423), the displacement of the wake can be seen in Fig. 7 at 20% channel height (near the hub). For ξ/h=6.25%, the wake center lies in the pitchwise measurement position of θ/θ_{stat}~0.36. When increasing the axial spacing to ξ/h=9.5%, the lowest stagnation location becomes θ/θ_{stat}~0.55-0.6. the wake position will then stabilizes for ξ/h=12.5% and ξ/h=18.75% at θ/θ_{stat}~0.45.

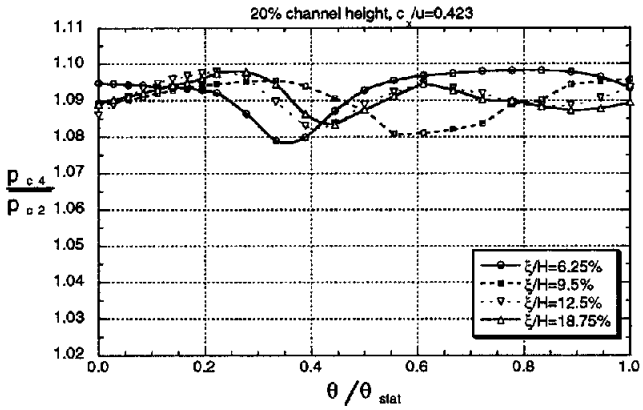

Fig. 7 Pitchwise distribution of the non-dimensional stagnation pressure at 20% channel height for the four axial spacing, at c_x/u=0.423

The displacement of the wake position between the cases of ξ/h=12.5% and ξ/h=9.5% is θ/θ_{stat}~0.15. A simple calculation shows that the corresponding flow angle for ξ/h=9.5% should be 39 degrees (Fig. 8). This is confirmed by the pitchwise distribution of the flow angle for the four axial spacings for high loaded conditions in Fig. 9.

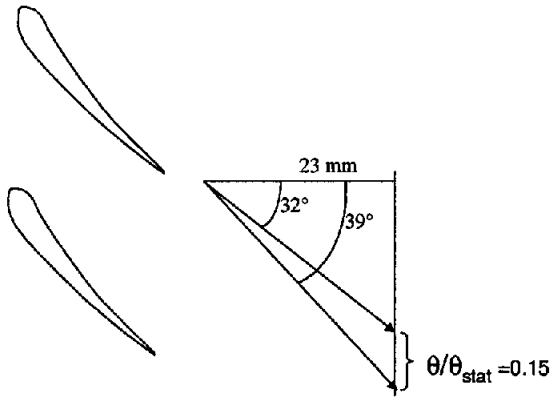

Fig. 8 Angle variation in the stator.

For flow conditions close to "design condition", the displacements of the wake with the axial spacing are less important but have the same tendency. Apart from the axial spacing of ξ/h=9.5%, the stagnation pressure distribution shows that the size of the wake is rather thin for high flow coefficients and becomes larger over the whole span as the loading increases. For the axial spacing of ξ/h=9.5% the wake is large at the tip for large flow coefficients. When the loading is increased, stagnation pressure profile shows that the wake widens at the hub and tightens at the tip to become of similar shape as the other cases (Fig. 11).

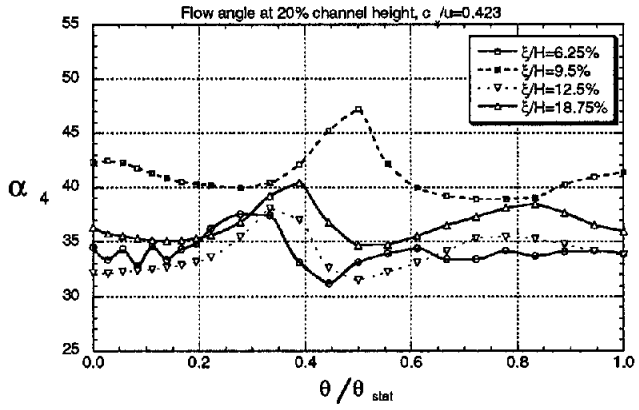

Fig. 9 Pitchwise distribution of the flow angle at z/h=20% for the four axial spacing, at $c_x/u=0.423$

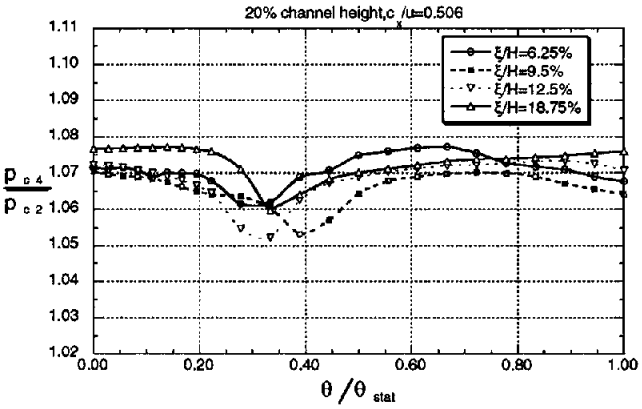

Fig. 10 Pitchwise distribution of the stagnation pressure at z/h=20% for the four axial spacing, at $c_x/u=0.506$

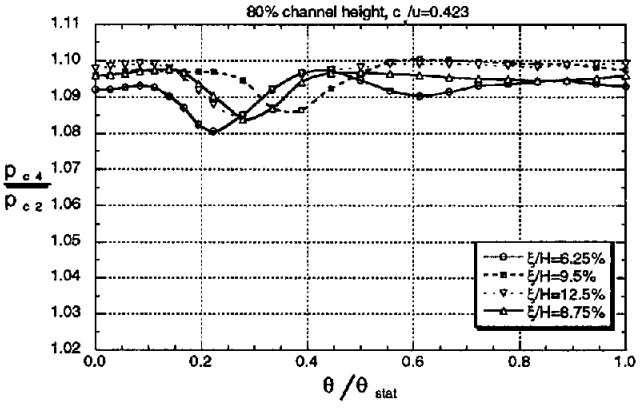

Fig. 11 Pitchwise distribution of the stagnation pressure at z/h=80% for the four axial spacing, at $c_x/u=0.423$

Blockage coefficient

The general form for the calculation of the blockage is the ration between the effective mass flow and the mass flow for free stream flow conditions.

$$B = 1 - \left(\int \rho c dA\right)_{actual} / \left(\int \rho c dA\right)_{inviscid}$$

Some arbitrariness exists concerning the definition of the free stream location, especially for tri-dimensional flows as in the compressor studied. This location was chosen at midspan, away from the stator wake.

The axial spacing plays a major role in the radial distribution of blockage coefficient and on the secondary flows (Fig. 12).

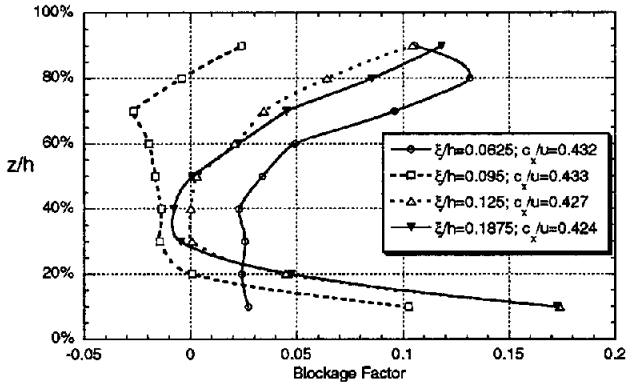

Fig. 12 Radial distribution of the blockage factor for low loaded conditions and for the four axial spacings

The sensitivity of the blockage factor is especially high between ξ/h=6.25% and ξ/h=9.5%. The similarity of the blockage factor between ξ/h=12.5% and 18.75% indicates that these axial spacings may have similar flows as can be seen in Fig. 13 which is the isentropic work reduced from the effective work.

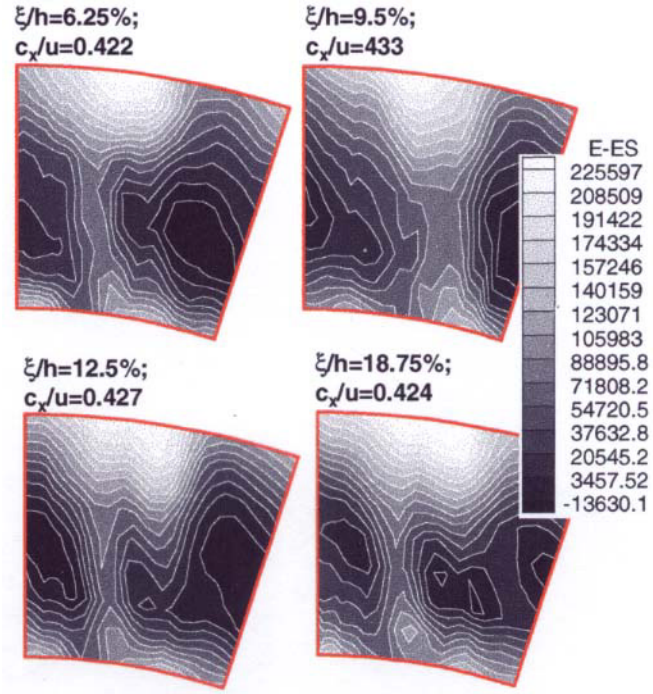

Fig. 13 Work lost per unit area for the four axial spacings and for high loaded conditions. [W/m^2]

It corresponds to the additional work due to the losses. This additional work is higher in the wake region for the two smallest axial spacings. The two other axial spacings show an increased additional work in the suction part side of the wake, near the casing. Even for a slightly higher flow coefficient, ξ/h=9.5% indicates higher losses in the wake regions. The displacement of the wake region towards the location where the free stream is defined explains the low and the negative values of the blockage factor for this axial spacing (Fig. 12).

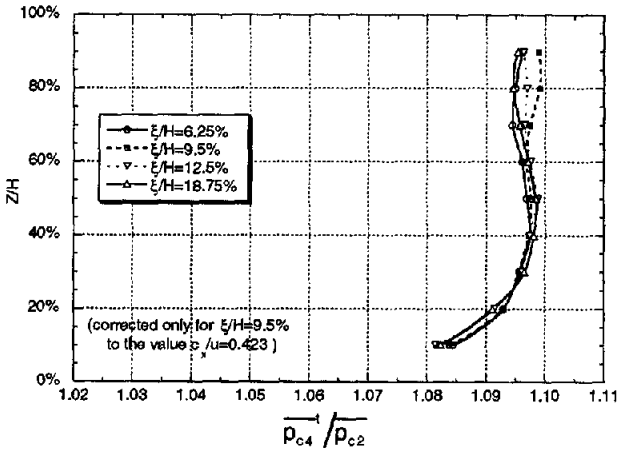

Fig. 14 Radial distribution of pitchwise averaged stagnation pressure for the 4 axial spacings; $c_x/u=0.423$

For flow coefficients superior to $c_x/u=0.44$, there are no significant differences in the radial distribution of the blockage factor. The radial distribution of the stagnation pressure seems also independent of the axial spacings for flow coefficients of $c_x/u=0.532$ and $c_x/u=0.507$ as can be seen in Fig. 15 and Fig. 16

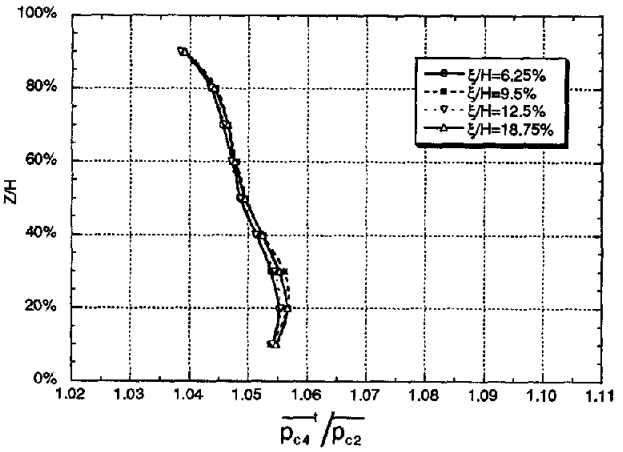

Fig. 15 Radial distribution of pitchwise averaged stagnation pressure for the 4 axial spacings; $c_x/u=0.532$

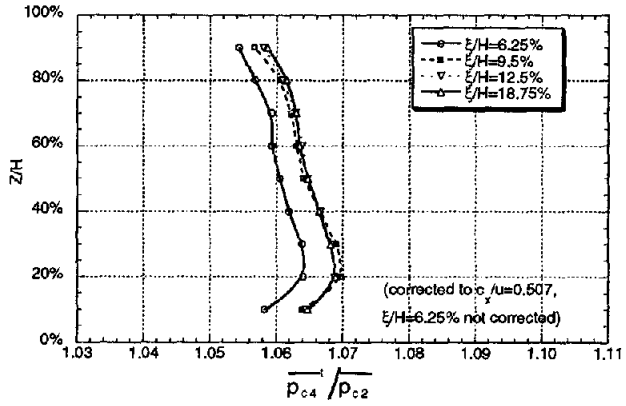

Fig. 16 Radial distribution of pitchwise averaged stagnation pressure for the 4 axial spacings; $c_x/u=0.506$

For high loaded conditions ($c_x/u=0.423$), particularly high values of the flow angle were measured for an axial spacing of ξ/h=9.5%. However, from hub up to the midspan region the radial distribution of the stagnation pressure ratio is rather similar to the other cases (Fig. 14), even though the two largest axial spacing seems to have lower values in the hub to 30% channel height.

Absolute Flow angle

From the flow angle taken from the measurements, ξ/h=9.5% shows a reduction of the surge limit and a deterioration of the flow for almost all the flow conditions.

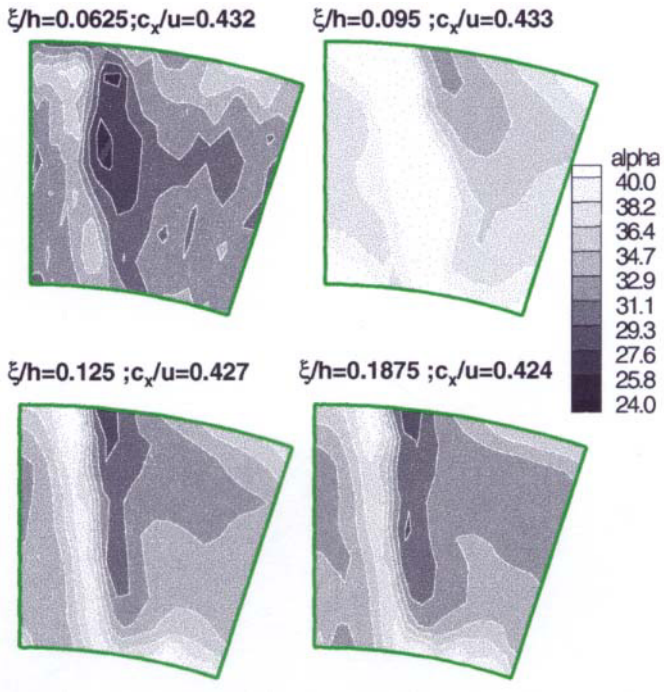

Fig. 17 Distribution of the flow angle in the measurement section 23 mm downstream of stator at c_x/u~0.43, and for the four axial spacings

Fig. 17 shows the distribution of the flow angles at the measurement location 84% axial chord downstream of the stator trailing edge, for c_x/u~0.43. These graphs clearly indicate an evolution of the flow with the axial spacing. For ξ/h=9.5%, the flow angle at this location is relatively high, typical of a blade boundary layer separation. For approximately the same flow coefficient, axial distances of ξ/h=12.5% and ξ/h=18.75% also show an increase of the flow angle, but only among a tight part of the wake (Fig. 17). Furthermore, the ξ/h=6.25% axial spacing case do not strongly separate for even higher loading at c_x/u=0.407.

From these measurements, it appears that the flow behavior can change with the axial spacing and with the loading. For the different axial spacings, the relative pitchwise position between the IGV and the stator were kept fixed. The stator was simply shifted upstream or downstream to obtain the desired axial distance. Fig. 18 indicates the positions of the stator and IGV blades upstream of the measurement locations in section 4. The IGV wakes are sketched in order to see their evolution through the rotor row. Positions of the Stator row are drawn for axial spacings of ξ/h=6.25%, ξ/h=12.5% and ξ/h=18.75%. The position of the IGV wake at the stator inlet varies with the axial spacing. The circumferential position of IGV wake at stator inlet has an influence on the characteristics of the compressor stage and on the flow itself. Furthermore for a given axial spacing the variation of the flow coefficient will have an impact on the velocity triangles, thus on the position of the IGV wake at stator inlet. The most detrimental conditions can be obtained if the IGV wake arrives on the suction side of the stator for high loaded conditions. One can imagine that ξ/h=9.5% axial spacing could fit these conditions. Thus the relative position between IGV and stator blades play a major role in the study of axial spacing between the blades.

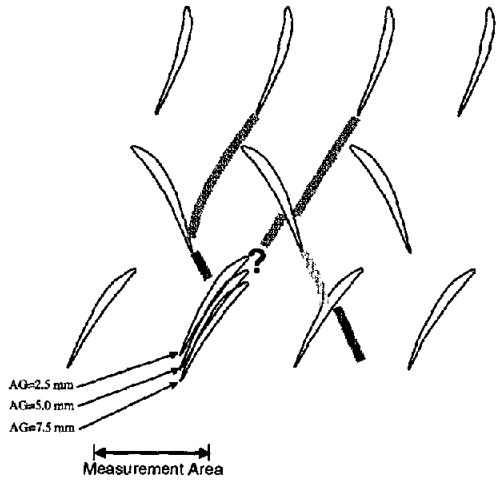

Fig. 18 Impact of IGV on the stator row

3.2 Detailed Pitot measurements

Pitot measurements downstream of the rotor

Fig. 19 shows the distribution of the stagnation pressure in section 3 (between rotor and stator) issued from the detailed Pitot probes measurements at design conditions (c_x/u=0.48). The presence of the IGV wake is still visible after having past the rotor row. In addition to the IGV wake, a second zone of high loss is visible close to the casing.

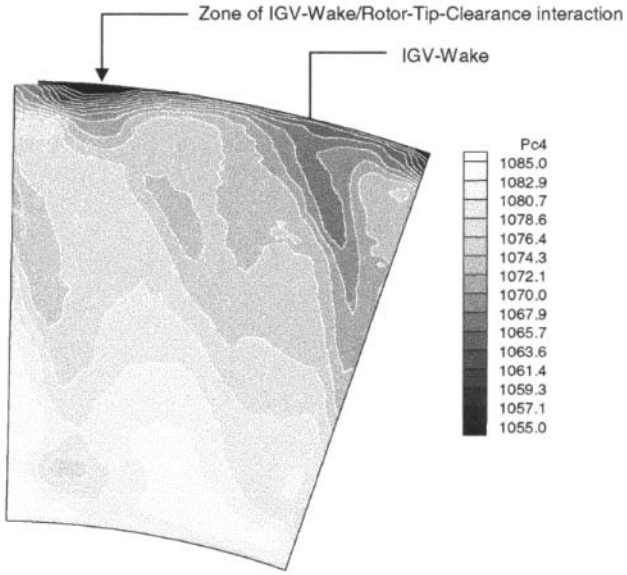

Fig. 19 Reduced stagnation pressure distribution in section 3; t/h=1.25%, ξ/h=12.5%

Hoynacki [ref. 7] made measurements downstream of a rotor, with presence of an upstream-IGV. The author indicates also that when the IGV wake arrives on the rotor tip vortex, this tip vortex will be split. The vortex turning in counter clockwise will be weakened. Hence in the absolute frame of reference, the flow field behind a rotor is not only non-axisymmetric because of the IGV wake, but also because of the rotor tip clearance. Indeed the second zone of loss corresponds to the described IGV wake/rotor-tip-clearance interaction. Hence, the flow arriving on the stator leading edge will depend of the upstream IGV pitchwise position.

Fig. 20 shows the pitchwise distribution of the static pressure downstream of the rotor at hub and casing. These measurements were done over a stator pitch () every one degree. These variations are induced by the potential flow due to the presence of the stator but also to the presence of the upstream IGV. Experimenters often use the wall pressure at a certain pitchwise location to determine the overall characteristics in multistage compressors. The obtained result

will depend of the relative pitchwise locations between the pressure tapping and the upstream stator blades.

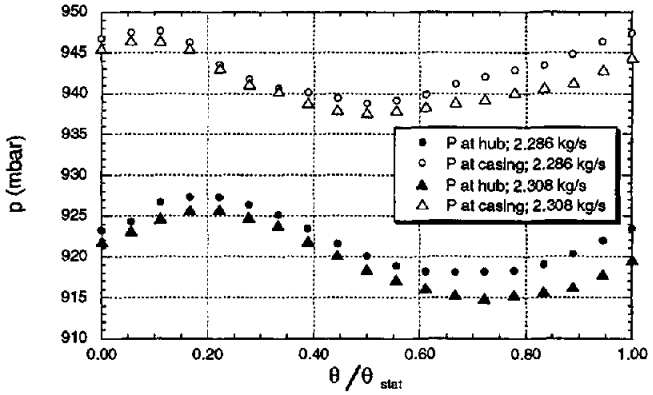

Fig. 20 Pitchwise distribution of the wall static pressures at hub and casing downstream of the rotor for two mass flows.

However this parameter has to be taken in account in the study of the axial spacing and of the indexing, especially when the wall pressure taps are used for determining the characteristics of a compressor. In fact, the upstream stator/IGV wake position will vary at trailing stator inlet, as seen in Fig. 25. Hence the wall static pressure will depend upon the flow phenomenon captured at the position where it is measured.

Detailed Pitot measurements downstream of the stator

Detailed Pitot measurements were performed 23 mm downstream of the stator trailing edge for the four investigated axial spacings. The flow coefficient was set to $c_x/u=0.48$. As mentioned before, the axial spacing between the rotor and the stator was varied by shifting the stator upstream or downstream. This means that the clocking between the stator and the IGV was not changed, for any axial spacing. The diameter of the cobra-Pitot- probe was 1 mm, thus the wall effects on the probe was reduced and the measured gradients could be caught. Fig. 24 shows the reduced stagnation pressure at the axial position of 84% axial chord downstream of the stator, for the studied axial spacings.

Due to the flow angle at rotor outlet, the IGV wake position and the zone of loss due to the rotor tip clearance moves in the clockwise when the axial spacing is varied, as can be seen in these graphical representations. The IGV wake regions that are associated with lower stagnation pressure are materialized by the dotted lines. The tip region is characterized by losses in stagnation pressure due to the second zone of losses seen in Fig. 19. This zone also moves in the clockwise direction. For an axial spacing of $\xi/h=6.25\%$, this zone lies in the suction side of the wake. For the axial spacings of $\xi/h=9.5\%$ this zone is aligned with the wake, but the IGV wake is less visible. However there is a large bubble of loss centered at 76% channel height. Near the hub, the IGV wake lies on the stator suction side. This creates a thickening of the stator wake. For the axial spacing of $\xi/h=12.5\%$ this low stagnation pressure zone at tip has increased in extend and in depth, and has moved to the pressure side of the wake. The bubble of loss decreased and below this zone, the wake has become thinner. When increasing the axial spacing to $\xi/h=18.75\%$, the tip loss zone entirely on the right side of the wake.

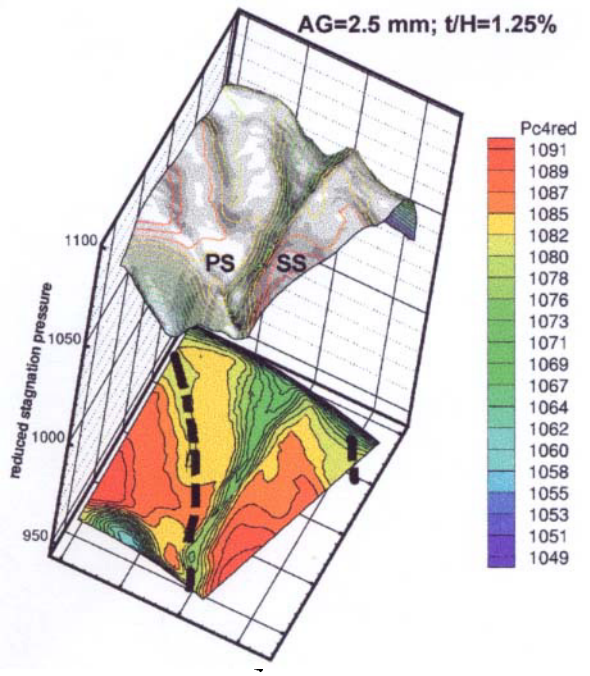

Fig. 21 Detailed pitot measurements of $P_{c4red;}$ t/h=1,25%, ξ/h=6.25%; c_x/u=0.48;

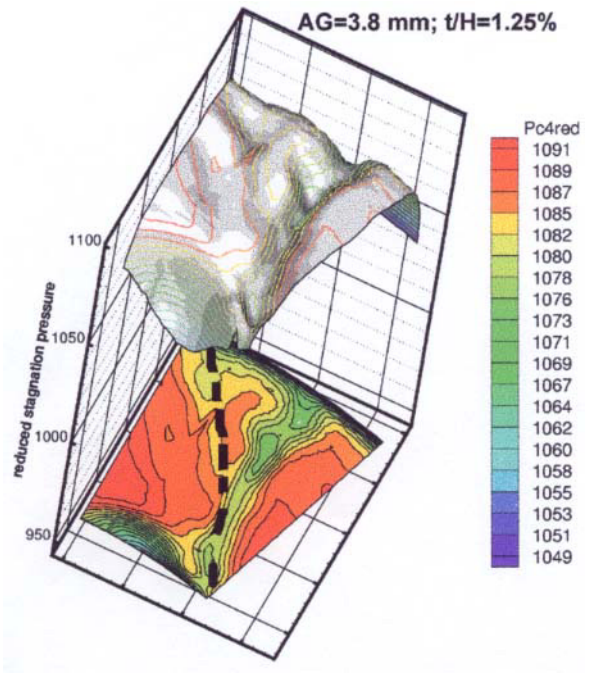

Fig. 22 Detailed pitot measurements of $P_{c4red;}$ t/h=1,25%, ξ/h=12.5%; c_x/u=0.48;

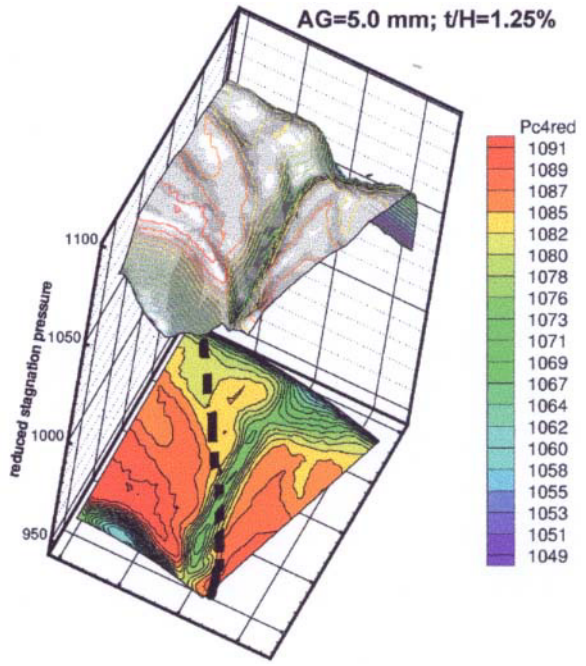

Fig. 23 Detailed pitot measurements of $P_{c4red;}$ t/h=1,25%, ξ/h=9.5%; c_x/u=0.48;

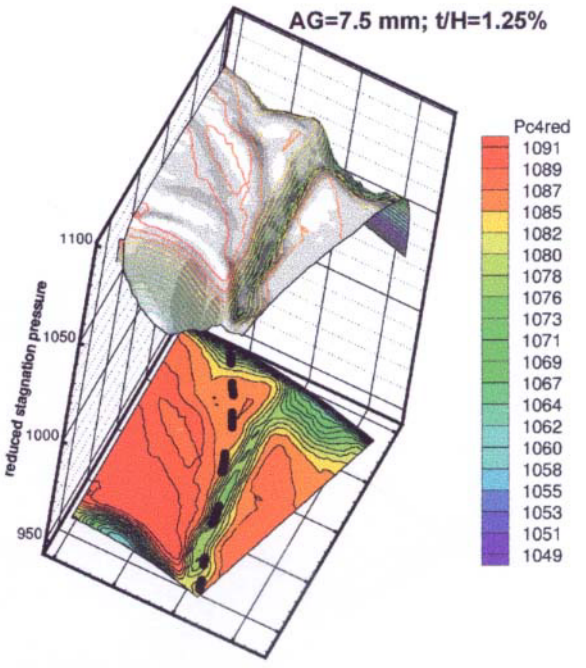

Fig. 24 Detailed pitot measurements of $P_{c4red;}$ t/h=1,25%, ξ/h=18.75%; c_x/u=0.48;

4. THE CLOCKING (OR INDEXING)

The investigation of the effect of the clocking was performed for an axial spacing of ξ/h=12.5% and for a tip clearance of t/h=1.25. in order to increase the effects of the secondary flows, the mass flow was set to 2.00 kg/s, which corresponds to a flow coefficient of 0.43. The clocking positions and the area averaged reduced stagnation pressure for each case are listed in Table 3. The position of the blades for the different clocking and the measurement location is drawn in Fig. 25.

Clocking	–0.45°	5.45°	7.45°	9.45°	11.45°
Test No	903	901	905	906	902
P_{c4red}	1104.89	1104.89	1102.81	1103.48	1103.28

Table 3 Test cases for the measurements

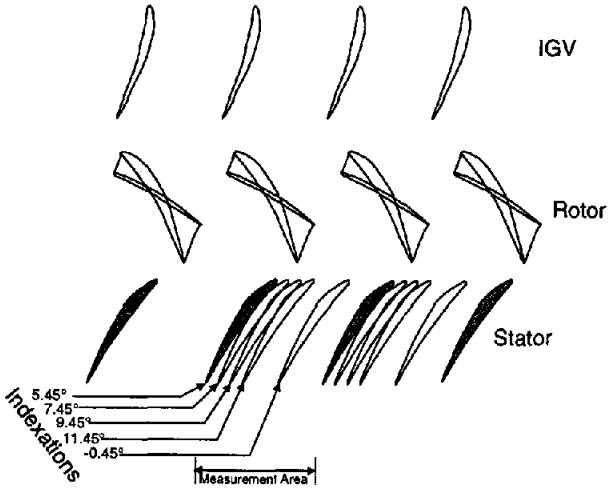

Fig. 25 Blade positions for the different clocking cases

The 0 degree clocking position corresponds to the relative pitchwise position between IGV and stator, used for the previous test cases (i.e. to the zero extension of the second hydraulic cylinder).

Fig. 26 represents the pitchwise distribution of the reduced stagnation pressures at respectively 20%, 50% and 80% channel height plotted over two pitches. The plots were adjusted in order to have the stator position fixed at a certain position and hence the stator wakes superposed on the plots. In the hub region (z/h=20%) and for an indexing of –0.45 degree, losses in stagnation pressure are noticed at the pressure side of the wake. This is caused by the presence of the IGV wake close to the stator wake, or by the fact that the IGV wake crosses the stator leading edge. For an indexing of 5.45 degree, the IGV wake has moved and is present on the suction side of the stator wake. Then the position of the IGV wake moves to the right (on the graph) with the clocking. In the midspan region, the circumferential motion of the IGV wake is characterized by a loss in stagnation pressure that moves to the left on the graph as the indexing is increased.

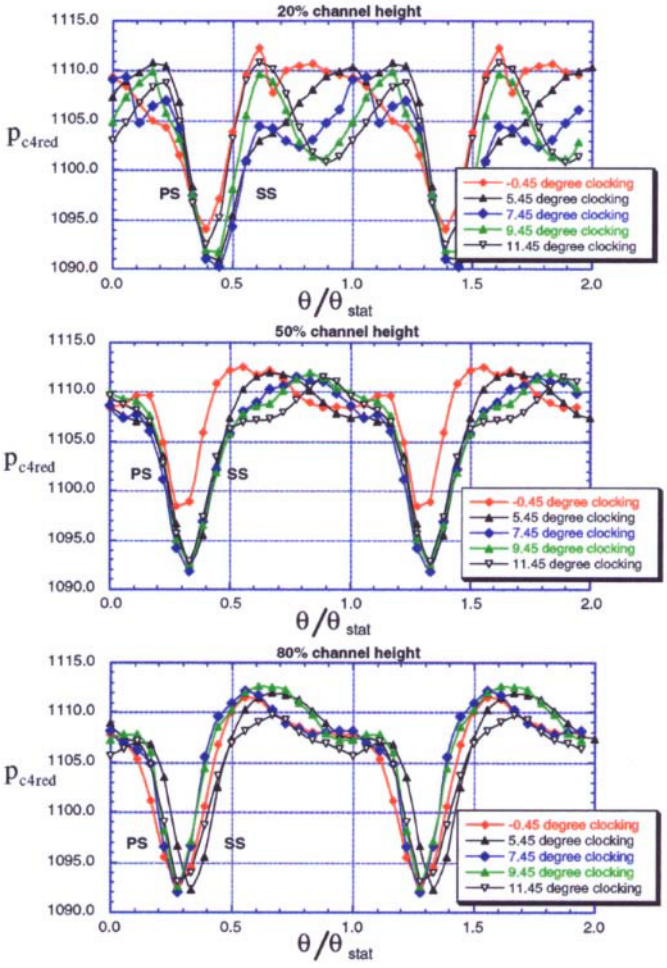

Fig. 26 Pitchwise distribution of the reduced stagnation pressure at z/h=20%, 50% and 80%, at 84% axial chord downstream of the stator, for the different indexings and for c_x/u=0.43 (ξ/h=12.5% and t/h=1.25%)

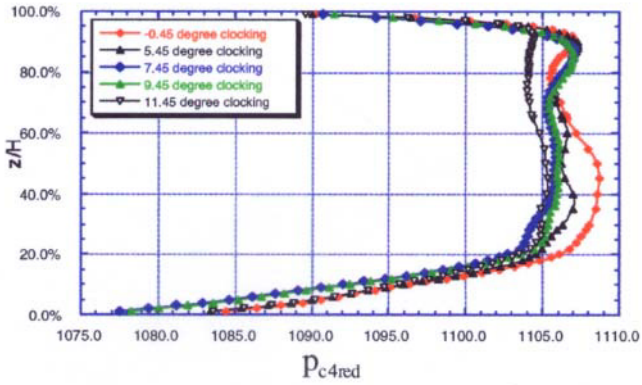

Fig. 27 Spanwise distribution of the pitchwise averaged reduced stagnation pressure (23 mm downstream of the stator trailing edge) for the different indexings (ξ/h=12.5% and t/h=1.25%)

For the indexing of –0.45 degree, the stator wake appears to be less deep and outside of the wake the stagnation pressure remains low, at the pressure side. For this case, the IGV wake impacts the pressure side of the stator in the midspan region and the overall stagnation pressure level is slightly higher than the other indexings as can be seen in Fig. 27.

In the tip region (z/h=80%), the stator wake does not seem to be strongly affected by the indexing. At design conditions it was seen in the measurements with the different axial spacings that a zone of loss issued from the interaction between the IGV wake and the rotor tip clearance vortex had an influence on the flow structure in the stator. For higher loaded conditions the flow downstream of the stator is not much affected by the circumferential variation of the low energy zones downstream of the rotor. One reason could be the higher velocities through the tip clearance due to stronger pressure gradients between suction side and pressure side of the rotor blade. These large velocities can be responsible of the wipe out of the regions of low energy.

Fig. 27 shows the radial distribution of the pitchwise area-averaged stagnation pressure issued from the detailed Pitot measurements for the five indexings. For the indexing of –0.45 degree, the reduced stagnation pressure is rather high up to 50% channel height. As seen before, this is due to the fact that the IGV wake flows onto the pressure side of the stator in this spanwise location. This improves the performances of the compressor. This behavior was also observed by Dorney et al. [*ref. 6*] on a low speed axial and by Barankiewicz et al. on a high speed axial compressor. For the indexing of 5.45 degrees, the IGV wake flows onto the leading edge of the stator and crosses the blade at about z/h=30%. This creates losses in stagnation pressure compared to the clocking of –0.45. For the indexings of 7.45 and 9.45 degrees, Fig. 26 showed the interaction between the IGV wake and the stator hub clearance. This effect leads to a lower stagnation pressure profile in the hub region. 11.45 degree clocking was the worst configuration because the IGV wake is present in the suction side at the tip of the stator and also in the stator hub corner vortex region. The stagnation pressure is the lowest in almost all the channel height.

5. CONCLUSIONS

The variation of the axial spacing between rotor and stator implies a variation of the position of the IGV wake at stator inlet. This is equivalent to vary the indexing between the IGV and the stator.

- The measurements for the different indexing positions show that at the location where the IGV crosses the stator blade is characterized by a thickening of the wake.
- The interaction between the IGV wake and the rotor tip clearance will create a zone of loss close to the casing at a certain location in the absolute frame of reference (Fig. 19). The position of this zone at stator inlet depends of the relative pitchwise position of the upstream IGV, and hence of the indexing between IGV and stator or as shown in this paper of the axial spacing between the blade rows. This zone will interact with the stator blade boundary layer. The worst deterioration of the flow in the tip region of the stator occurred when this low energy fluid arrives on the stator suction side.
- The loss in stagnation pressure in the stator hub clearance vortex is strongly influenced by the presence of the IGV wake. The Pitot measurements, downstream of the stator show that the hub clearance vortex losses increase in extent and in magnitude in presence of the IGV wake. Hence the losses in the hub region are dependent on the indexing and on the axial distance between the blade rows.

The most important contribution to the variation of performances with indexing or with the axial spacing are due to the secondary flows near the endwalls and especially to the rotor tip and stator hub clearances. In this study, the flow at stator inlet is characterized by the presence of the IGV wake, and by a zone of loss coming from the interaction between the IGV wake and the rotor tip clearance. The circumferential position of these low energy zones will determine the structure of the flow in the stator passage and hence the performance of the compressor stage. A variation of more than 3 percent-points in efficiency was measured when varying the axial distance between rotor and stator. In a multistage axial compressor, the variation of the axial spacing does not only implies the variation of the indexing between the stator, but also between the rotors.

REFERENCES

ref. 1 Smith Jr L.H., 1969, Casing Boundary Layers in Multistage Axial-Flow Compressors, Proceeding of the Symposium on Flow Research on Blading, BBC Limited, Switzerland, p. 275-304,

ref. 2 Mikolajczack A.A., 1975, The Practical Importance of Unsteady Flow, AGARD-CP-177, Vol. 177

ref. 3 Hetherington R., Moritz R.R., 1975, Influence of Unsteady Flow Phenomena on the Design and Operation of Aero Engines, AGARD-CP-177, Vol. 177

ref. 4 Cumpsty N.A., 1989, Compressor aerodynamics, Book, Published by Longham Scientific & Technical.

ref. 5 Barankiewicz W.S., Hathaway M.D., 1997, Effects of Stator indexing on performance in a Low Speed Multistage Axial Compressor, 97-GT-496.

ref. 6 Dorney D.J., Sharma O.P., Gundy-Burlet K.L., 1998, Physics of Airfoil Clocking in a High speed Axial Compressor, 98-GT-82

ref. 7 Hoynacki A., Stuffeninteraktion, 1999, Vorhaben Nr. 601, Heft 679-1999, Forschungsvereinigung Verbrennungsmaschinen e.V. Frankfurt am Main.

ref. 8 hubert F.W., Johnson P.D., Sharma O.P., Staubach J.B., Gaddis S.W., 1996, Performance improvement Through Indexing of Turbine Airfoils: Part 1-Experimental

investigation, Journal of Turbomachinery, vol. 118, pp 630-635.

ref. 9 hubert F.W., Johnson P.D., Sharma O.P., Staubach J.B., Gaddis S.W., 1996, Performance improvement Through Indexing of Turbine Airfoils: Part 2-Numerical Simulation, Journal of Turbomachinery, vol. 118, pp 630-635.

ref. 10 Griffin L.W., hubert F.W., Sharma O.P., 1996, Performance improvement Through Indexing of Turbine Airfoils: Part 2-Numerical Simulation, Journal of Turbomachinery, vol. 118, pp 636-642.